ELSEVIER

Biochimica et Biophysica Acta 1195 (1994) 1–10

BBA Biochimica et Biophysica Acta

A computer simulation study of the relation between lipid and probe behaviour in bilayer systems

Uulke A. van der Heide, Yehudi K. Levine *

Debye Research Institute and Department of Molecular Biophysics, Buys Ballot Laboratory, University of Utrecht, P.O. Box 80.000, 3508 TA Utrecht, The Netherlands

Received 28 February 1994

Abstract

Computer simulations are presented of the behaviour of elongated probe molecules anchored to the interface of lipid bilayers above the phase transition of the hydrocarbon chains. The simulations thus mimic the behaviour of the fluorescent probe 1-(4-(trimethylammonio)phenyl)-6-phenyl-1,3,5-hexatriene (TMA-DPH) and Cholestane spin label in lipid systems. In contrast to any experimental technique the simulations follow the behaviour of both the lipid molecules and the probe within the bilayer structure. Thus, the relation between the behaviour of the probe molecules and the order and dynamics of the lipid chains can be studied in detail. We find that the presence of probe molecules, at the low concentrations used experimentally, causes only a marginal perturbation in the intrinsic properties of the lipid chains. The simulations presented support the conventional prescription for describing the orientational behaviour of probe molecules in lipid bilayers in terms of a local effective orienting potential. They indicate, however, that the potential arises from the confinement of the probe molecules between long segments of lipid chains in elongated free-volume cavities within the bilayer structure. In this sense the orienting potential concept needs to be refined in order to take into account the combined effect of the restricted free rattling motions of the probes within the free-volume cavities and the orientations of the cavities themselves relative to the normal to the bilayer plane. The time scale of the motions of the cavities within the bilayer is determined by the rotational motions of long segments of the lipid chains. These observations justify the use of rigid probe molecules such as TMA-DPH and Cholestane spin labels for monitoring the orientational order and dynamics in lipid bilayer systems.

Keywords: Lipid bilayer; Computer simulation; Monte Carlo method; Membrane dynamics

1. Introduction

Probe techniques such as fluorescence depolarization and ESR spectroscopy are widely used for the study of the orientational order and rotational dynamics in membrane systems. The experiments monitor the behaviour of extraneous probe molecules embedded in the membrane structure at the smallest possible concentration compatible with an acceptable signal/noise ratio. The starting point in the description of the experimental observations, is a model for the orientational order and rotational dynamics of the probe in the membrane system. To this end, it is common to assume that each probe molecule experiences a local orienting potential imposed on it by the surrounding lipid molecules [1–5]. The orientational distribution function of the molecules relative to the normal to the bilayer surface is given simply by the Boltzmann distribution corresponding to this orienting potential.

It has become routine practice to apply the 'wobble-in-cone' model postulated by Kinosita et al. [6,7] for the interpretation of fluorescence depolarization experiments. On the other hand, the Brownian rotational diffusion (BRD) model [2] has been widely used for simulations of ESR spectral lineshapes as well as for the analysis of fluorescence anisotropy decays. The only difference between these models is the form of the orienting potential acting on the molecules. The 'wobble-in-cone' model assumes the simplest form of the potential, a square well with infinite walls at an

* Corresponding author. Fax +31 30 532706

SSDI 0005-2736(94)00154-H

arbitrary angle β_0, where $0 \leq \beta_0 \leq \pi/2$. On the other hand the BRD model utilizes the potential $U(\beta)$

$$U(\beta) = -kT(\lambda_2 P_2(\beta) + \lambda_4 P_4(\beta)) \quad (1)$$

where P_L is the Legendre polynomial of rank L and β is the angle made between the long axis of the probe and the normal to the local membrane surface. This choice of the potential is based on the observation that only the order parameters $\langle P_2 \rangle$ and $\langle P_4 \rangle$ can in principle be obtained from the experiment in a model-independent way. In both models the long axis of the probe is assumed to undergo small stochastic angular steps subject to the orienting potential.

We have recently proposed an alternative description of the motion of a probe in a membrane system, the Compound Motion (CM) Model, for the analysis of fluorescence depolarization experiments [8,9]. Here the probe molecules undergo fast, though restricted local motions within a slowly rotating cavity in the lipid bilayer structure. The cavity may be envisaged as the free volume between the lipid molecules, so that its position and orientation changes with the internal conformational motions of the lipid chains.

The tacit assumption underlying this approach is that the behaviour of the probes reflect the intrinsic behaviour of the indigenous lipid molecules. In addition, the probes are assumed to have no specific interaction with the lipid molecules (ideal mixing). However, thus far no explicit link has been found between the order parameters and rotational rates extracted from the models and the dynamic structure of the lipid matrix. Moreover, it has been argued that the information obtained from membrane systems with probe techniques is compromised by structural perturbations caused by the incorporation of the probe molecules. The question now arises as to what information is furnished by probe techniques about the membrane system. In particular, it is important to understand the factors governing the orientational order and rotational dynamics of the probes in the lipid matrix.

A better insight into the information provided by probe techniques about membrane systems, can be gained using computer simulation techniques. In contrast to any experimental technique the simulations follow the behaviour of both the lipid molecules and the probe within the bilayer structure. Thus, the relation between the behaviour of the probe molecules and the order and dynamics of the lipid chains can be studied in detail. Moreover, the simulations afford a direct comparison between the local information revealed about the order of C–D bonds along the chains by ^{2}H-NMR experiments and the orientational behaviour of long chain segments in the bilayer. In this way the simulations can be used to relate experimental data obtained from selective experiments such as NMR and from probe molecule techniques. An added advantage of this approach is that it visualizes the effects of the incorporation of probe molecules on the order and dynamics of the lipid molecules.

We have recently shown that Monte Carlo dynamics (MCD) methods can be used to simulate the principal structural features of lipid bilayers [10–13]. The underlying premise of the MCD method is that the conformational dynamics of the lipid chains can be described as the superposition of local structural rearrangements involving small chain segments. This is realized in a computationally efficient way by making use of a lattice. The MCD calculations were implemented taking into account only the conformational energy of the chains and excluded volume effects. The simulations reproduced the electron density profile of the bilayers obtained from X-ray diffraction experiments, the ^{2}H-NMR order parameter profile of the C–D bonds along lipid chains as well as their mobility gradient. In addition, the simulations accounted for the effects of cholesterol molecules on the conformational order and dynamics of the lipid molecules.

Here we have used the MCD technique for simulating the behaviour of elongated probe molecules anchored to the interface of lipid bilayers above the phase transition of the hydrocarbon chains. Ideal mixing was ensured by incorporating only excluded volume interactions between the probe molecules and the lipid chains in the calculations. The simulations thus mimic the behaviour of the fluorescent probe TMA-DPH and Cholestane spin label in lipid systems. The simulations follow simultaneously the conformational fluctuations of the lipid chains and the rotational motions of the probe molecules between them. We find that the presence of probe molecules causes only a marginal perturbation in the intrinsic properties of the lipid chains. The simulations indicate furthermore, that the orientational order and rotational rates of the probe molecules are determined to a large extent by the fluctuations in the free-volume cavities of the bilayer structure. Importantly, the orientational order and the timescale of the tumbling motion of the long molecular axis is found to reflect that for long chain segments in the bilayer structure.

2. Method of simulation

The Monte Carlo (MCD) technique for simulating the dynamic behaviour of hydrocarbon chains of lipids in monolayer and bilayer structures has been discussed and validated in detail previously [10–13] and only the salient points will be summarized here.

The method makes use of a representation of hydrocarbon chains, both saturated and *cis* unsaturated bonds, on a cubic lattice. The bilayer was constructed of two monolayers each containing 64 model lipid

chains and a single rigid probe. A unified atom representation was used, with the first 'headgroup' atom of each chain being dressed with a larger excluded volume envelope than the atoms depicting the methylene groups. The bilayer was contained in a Monte Carlo box having a square cross-section in the XY-plane of the lattice and extending along the positive Z-axis. The impenetrable interfaces of the monolayers forming the bilayer system were taken to lie parallel to the XY-plane of the lattice, at heights $Z = 0$ and $Z = T_{bil}$, with T_{bil} the bilayer thickness. The molecules were attached to the interfaces with the first atom being allowed to move vertically by two lattice units. Periodic boundary conditions were imposed on the positions of all the beads in the XY-plane only.

The conformational dynamics of the lipid chain is considered to arise from a superposition of local structural rearrangements constrained by the bond lengths. For example, in a polymethylene chain the elementary move involves the transfer of a pair of adjacent atoms, $-C_1-C_2-$, chosen at random to different lattice sites. Cooperative moves involving 6 atoms are invoked to account for the motion of the rigid unsaturated chain segments. The first and last bonds are allowed to undertake random orientations. The lack of restrictions on the positions of the first 'headgroup' atoms in the XY-plane resulted in a lateral translational motion of the chains across that plane.

Each random elementary move attempted by the atoms is subjected to three acceptance tests:

(1) A move is only accepted if the final lattice positions of the dressed atoms are unoccupied.

(2) The new configuration was accepted with a probability P given by the symmetric scheme:

$$P = \exp(-E_{new}/kT) \,/\left(\exp(-E_{old}/kT) + \exp(-E_{new}/kT)\right)$$

This test is convenient as it is determined by the differences in the torsional energy involved in the move, rather than by absolute values.

(3) Chain configurations with g^+g^- or g^-g^+ conformations about adjacent bonds are rejected.

The Monte Carlo dynamics algorithm for a bilayer containing M hydrocarbon chains each consisting of N atoms was executed in the following way. Given a particular configuration of the bilayer, Ω_j, $M \times N$ local conformational moves are attempted at random with each atom in the system having an equal chance of being picked. These $M \times N$ moves generate a new configuration of the bilayer, Ω_{j+1}. The cycle is now repeated using Ω_{j+1} as the starting configuration. The fundamental time-step of the algorithm is defined as the time required for the bilayer to undergo a transition from configuration Ω_j to Ω_{j+1}. It is important to realize that this time step of the MCD algorithm cannot be related to an absolute scale [27].

The probe molecules were represented as rigid, solid objects 21 (or less) lattice units long. Their cross-section was taken to be a square with a side of five lattice units. The molecules are anchored to the bilayer interface at one end and allowed to undergo random rotational and translational motions. The moves were subjected to a single acceptance test, namely that the final lattice positions were unoccupied.

The vertical translational motions were restricted to three lattice units relative to the bilayer interfaces, but no restrictions were placed on their lateral motions in the XY-plane. The detailed implementation of the small angular excursions of the long molecular axes about the anchor point were described previously [10]. Essentially, the long axis of each molecule was represented by a vector whose tip was allowed to jump over all the lattice points enclosed in a spherical shell with an internal radius of 35 lattice units and an external radius of $(36^2 - 1)^{\frac{1}{2}}$ units. The internal radius was chosen as a compromise between computer memory requirements and a smooth distribution of vector orientations. The jumps were restricted in size by limiting the linear displacement of the tip to less than five lattice units. This procedure is advantageous in that it can be used to implement the orientational motions of a probe molecule of arbitrary length. The random orientational motion of the vector tip over the shell reproduced the mono-exponential decay of the time correlation functions expected for isotropic diffusion. Additional tests showed the decay of this correlation function obtained on subjecting the motion of the vectors to an orienting potential, was in excellent agreement with that obtained from the BRD model with the same potential.

The algorithm of the simulations of bilayer containing probe molecules is similar to the one described above for the lipid chains. Now a move of each probe molecule is attempted once every simulation cycle leading to a new bilayer configuration.

We have typically generated a trajectory consisting of $8 \cdot 10^4$ bilayer configurations each separated by 10 elementary time-steps at a temperature of 330 K. The calculation for a bilayer of 126 chains each consisting of 18 atoms and 2 probe molecules required around 36 hours on a DEC3100 workstation. With this choice, the statistical fluctuations in the calculated order parameters for the probe molecules and chains obtained from runs starting with different initial bilayer configurations varied by less than 3%. Furthermore, the decay of the time correlation functions for every atom of the chain and for the long axis of the probe molecules was found to be independent of the sampling frequency of the trajectory generated. The only caveat being that the total time of the trajectory used for the evaluation of the correlation functions must be long compared to the decay time of the slowest decay component.

In order to characterize the rotational motions of the probe molecules we have used the trajectories to evaluate three orientational time correlation functions $G_{k0}(t)$, $k = 0,1,2$

$$G_{k0}(t) = \langle\langle D^2_{k0}(\Omega_{BM0}) D^{2*}_{k0}(\Omega_{BMt})\rangle\rangle \quad (2)$$

Here D^L_{mn} are Wigner rotation matrix elements [14] and Ω_{BM0} and Ω_{BMt} denote respectively the orientation of the Z-axis of the probe molecule at time $t = 0$ and t, respectively, in the bilayer frame. The double bracket indicates an average over the probe or lipid molecules. The amplitudes of the orientational correlation functions at time $t = 0$ can be expressed as linear combinations of the order parameters $\langle P_2\rangle$ and $\langle P_4\rangle$ in a model-independent way. These time-correlation functions were fitted to the predictions of the 'wobble-in-cone', BRD and CM models using a non-linear Marquardt optimization procedure. It will also prove convenient when dealing with the motion of long chain segments to consider the total time correlation function $G_0(t)$:

$$G_0(t) = G_{00}(t) + 2G_{10}(t) + 2G_{20}(t) \quad (3)$$

We note that this correlation function is the fluorescence anisotropy decay measured in vesicle systems [1].

3. Results and discussion

3.1. Pure lipid bilayers – equilibrium properties

MCD simulations were carried out in order to model the behaviour of bilayers of four different lipids: dimyristoylphosphatidylcholine (DMPC), dipalmitoylphosphatidylcholine (DPPC), palmitoyloleoylphosphatidylcholine (POPC) and dioleoylphosphatidylcholine (DOPC) at 330 K, above the phase transition temperature of their hydrocarbon chains. Only the intramolecular torsional potentials and excluded volume interactions were implemented. The simulations were performed on varying the side of the Monte Carlo box in the XY-plane from 54 to 72 lattice units at a constant temperature. In this way the effective area of each of the 128 lipid chains was changed over a wide range. The order parameters S,

$$S = \tfrac{1}{2}\langle 3\cos^2\beta - 1\rangle$$

of the C–D bonds of the lipid chains were found to decrease on increasing the side of the Monte Carlo box, in agreement with experimental data [15–17]. Here β denotes the angle between the C–D vector and the normal to the bilayer interfaces, the lattice Z-axis. It now needs to be recognized that the C–D vector in a saturated hydrocarbon chain is oriented tetrahedrally relative to the plane defined by the sp^3-sp^3 bonds attached to the atom. On the other hand, the C–D

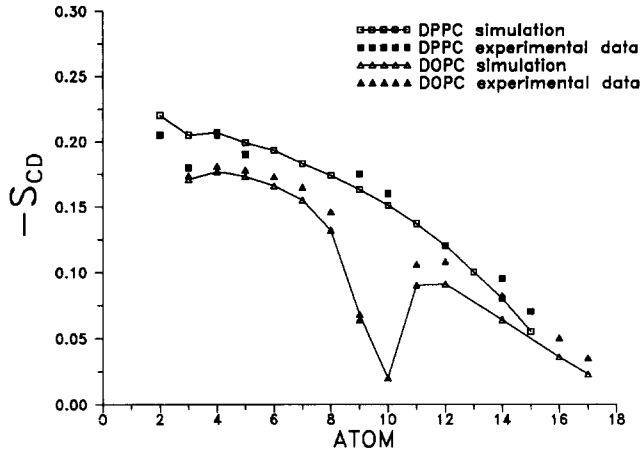

Fig. 1. A comparison of the order parameter profile of C–D bonds along the hydrocarbon chains in bilayers of DPPC and DOPC measured in ^{2}H-NMR experiments and simulated using MCD.

vectors attached to a carbon atom of the unsaturated *cis* segment lie in the plane defined by the sp^3-sp^2 bonds [11,12]. We note that the order parameters S of the C–D bonds are negative since they exhibit a preferential orientation in the XY-plane.

We have found that the order parameter profile of the C–D bonds in DPPC in a box of side 54 lattice units in the XY-plane (Fig. 1), tracks well the experimental profile observed using ^{2}H-NMR. We note that as all the hydrocarbon chains are considered to be equivalent in our formulation, the simulations do not reproduce the experimental differences between the ordering of the two hydrocarbon chains of a lipid molecule near the carboxyl groups. In order to reproduce the lower experimental order parameter profile for bilayers of DOPC (Fig. 1), the side of the Monte Carlo box was increased to 62 lattice units. The higher area per chain for the unsaturated bilayer systems has been observed experimentally [18–21]. The combination of a high degree of alignment along the bilayer normal and the planar sp^2 geometry of the *cis* segment result in the order paramater anomaly for the C–D bonds at positions 9 and 10 in the DOPC chains (Fig. 1), [11,22]. Simulations of DMPC and POPC bilayers were carried out for a Monte Carlo box of side 54 and 60 lattice units, respectively.

The orientational order of the C–D vectors is also reflected in the preferential alignment of the end-to-end vectors of the chains in a direction parallel to the bilayer normal. The order parameter of this vector for DOPC bilayers ≈ 0.6 is significantly higher than that for the DPPC bilayers ≈ 0.5. This simply reflects the high degree of alignment of the rigid *cis* unsaturated segment along the bilayer normal [11,22]. The order parameter for the central $C_9 = C_{10}$ bond of the *cis* segment, $S \approx 0.37$ in egg lecithin bilayers obtained form infra-red dichroism experiments [23], is in good agree-

ment with a value of ≈ 0.35 found in the simulations of POPC and DOPC bilayers. This is considerably higher than the value $S \approx 0.15$ found in the simulations for the corresponding bond in the saturated chains of DMPC, DPPC and POPC.

3.2. Probes in lipid bilayers – equilibrium properties

One probe molecule was now introduced into each monolayer containing 32 lipid molecules. This effective molecular ratio is significantly higher than that used experimentally (about 1:250). This high ratio was used with the sole object of keeping the simulation time within reasonable bounds. Simulations for a DPPC bilayer were now carried out as a function of the length of the model probe molecule. Probe molecules less than 11 lattice units long showed no significant orientational order with a low order parameter S for their Z-axes. It is important to note here that such a distribution simply implies an equal distribution of the long molecular axes over the surface of a sphere whose pole axis is the normal to the bilayer surface. Consequently, significantly less molecules will be oriented parallel to the normal to the bilayer, than in a direction perpendicular to it.

The probe molecules start to exhibit substantial orientational order only on increasing their length to 15 lattice units and above. Indeed, the experimental values for the order parameters, $S \approx 0.6$, found for TMA-DPH and Cholestane spin labels are obtained for probes 21 lattice units long. We shall henceforth only consider probes of this length since the simulations showed that their order parameters, $S = 0.66$, 0.51 and 0.48 in bilayers of DMPC, POPC and DOPC, respectively, are in good agreement with those found for TMA-DPH and Cholestane spin labels in oriented bilayer systems [24].

The number density of probes relative to the bilayer normal for DMPC bilayers is shown in Fig. 2. The number density simply gives the fractional number of times the Z-axis of the probe is found at a given angle β with respect to the normal to the monolayer surface during the simulation. We note that the number density is identical for each monolayer on taking the normal to be pointing outwards towards the water phase. The number density for the bilayer as a whole can be obtained by reflecting that shown in Fig. 2 about $\beta = \pi/2$. Conventionally, the orientational distribution function $f(\beta)$ is presented rather than the number density $n(\beta)$. However, the two are related simply as $n(\beta) = f(\beta)\sin\beta$. The general form of the number density reflects the fact that the probe axes are actually distributed over the surface of a sphere and in no way implies a collective molecular tilt relative to the bilayer normal.

The number density distribution can be seen to

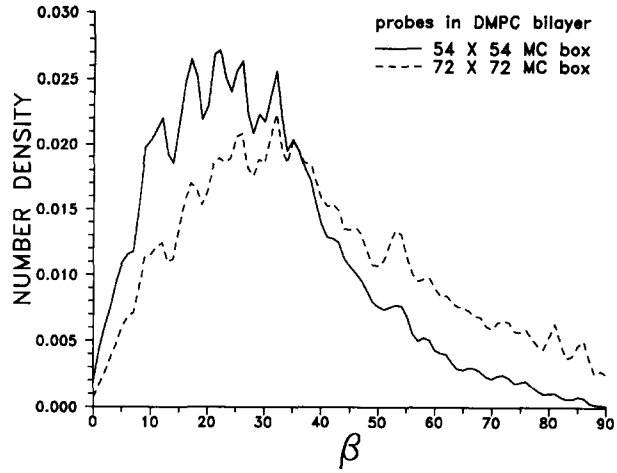

Fig. 2. The fractional number of times (number density) the long axis of an anchored probe molecule is encountered at an angle β relative to the bilayer normal along the trajectory obtained from MCD simulations. The number densities for the two monolayers have been combined by reflection about the symmetry plane at $\beta = \pi/2$. The oscillations are caused by the underlying lattice used in implementing the rotational jumps.

broaden and moreover to shift towards higher angles on increasing the side of the Monte Carlo box from 54 to 72 lattice units (Fig. 2). This change corresponds to a reduction in the order parameter of the probe from 0.66 to 0.42. A concomitant reduction is observed in the order parameters of both the C–D bonds over the length of the hydrocarbon chains and the end-to-end chain vectors.

We shall now address the question as to why short probe molecules are not oriented by the lipid matrix, while long probe molecules exhibit a high orientational alignment relative to the normal to the bilayer plane. We have shown previously, that the lipid chains are considerably disordered, with any atom in a molecule having a small, but finite, probability of reaching the impenetrable bilayer interface [10,11]. As a result of this conformational flexibility, the density of chain packing varies across the thickness of the bilayer. The packing density is highest near the impenetrable interface, but is significantly lower near the middle of the bilayer where both monolayers make contact [10]. This finding now provides a framework for explaining the observed length-dependence of the orientational behaviour of the probe molecules. The short probe molecules can be accommodated easily within free-volume cavities in the bilayer structure. However, these cavities are either too small or do not have a simple geometrical form for containing the long probe molecules. Consequently, the rotational motions of the long probe molecules are determined by the availability of large free-volume cavities created by the conformational motions of the lipid chains. Such large cavities are more likely to exist in a direction parallel to long

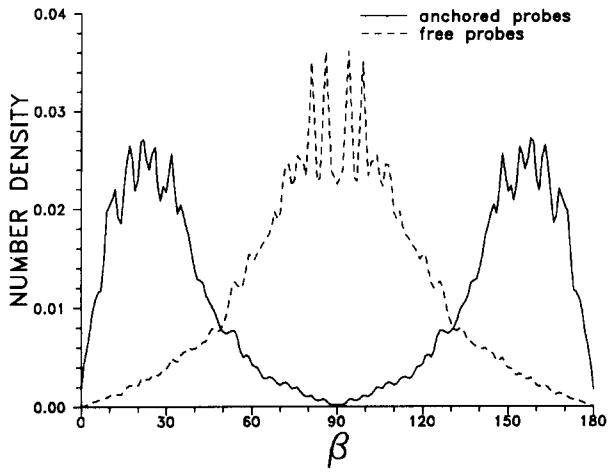

Fig. 3. The fractional number of times (number density) the long axis of a probe molecule is encountered at an angle β relative to the bilayer normal along a trajectory obtained from the MCD simulations for probe molecules anchored to the aqueous interfaces of a DPPC bilayer and free to move within the structure. The oscillations are caused by the underlying lattice in used in implementing the rotational jumps.

segments of hydrocarbon chains than across them, in a direction parallel to the bilayer surface. As the long chain segments lie on average perpendicular to the bilayer surface, we expect the long probe molecules to exhibit a preferential orientation along the normal to the bilayer. Indeed, the order parameters for the end-to-end vectors of the saturated chains in DMPC, DPPC and POPC bilayers are some 10–15% higher than the order parameters of the probe molecules, in agreement with our working hypothesis. On the other hand, the order parameters of the end-to-end-vectors of the unsaturated chains in the POPC and DOPC bilayer systems, $S \approx 0.6$, are significantly higher than those reported by the probe molecules. This discrepancy, however, only arises for chain vectors spanning the central *cis* unsaturated segment of the chain. The order parameters for the two saturated chain segments encompassing atoms 2–8 and 11–18 of the unsaturated chains are similar to those found for the probe molecules. It thus appears that the probe molecules do not monitor the high orientational order of the *cis* unsaturated segment, but are rather influenced by the conformationally disordered chain segments.

The picture of free-volume cavities as the operative mechanism for determining the orientational order of the probes is further supported by the observed orientational behaviour of long probe molecules free to move within the bilayer structure (Fig. 3). The free molecules migrate towards the centre of the bilayer, where the density of free-volume cavities is highest. The low packing density of the chains in the centre of the bilayer arises from the imperfect stacking of the two opposing monolayers. The molecules are now oriented with their long axes parallel to the bilayer surface, rather than perpendicular to it. Interestingly, long carotinoid molecules have been found to be oriented in this way in lipid bilayer systems [25,26].

The hypothesis of free-volume cavities for explaining the orientational behaviour of the probes proposed here implies that the orientational behaviour observed is determined by the ratio of the length of the probe to the average length of the lipid chain. This view is corroborated by the observation that the order parameter of probes of length 21 lattice units is higher in DMPC bilayers than in the corresponding DPPC system, even for identical levels of the plateaus of the order parameter profiles.

The simulations show that the order parameter of the long axes of the probe molecule can be related to the average orientational behaviour of the lipid chains. This behaviour is manifested by the order parameter profile of the C–D bonds revealed by ^{2}H-NMR experiments [15–17]. Our simulations thus indicate that the order parameter profile drops to lower levels on increasing the effective area per molecule. Consequently, the reduction in the order parameters found for the probe molecules in the sequence DPPC > POPC > DOPC, appears to be a reflection of the increase in the area per lipid molecule in these bilayer systems [18–21].

3.3. Perturbation of bilayer by probe molecules

The order parameter profiles for the C–D bonds of the lipid chains in the presence of 1 probe per 32 lipid molecules, are the same as those found for the pure DMPC and DPPC bilayers within the level of the statistical uncertainties of 3%. A small increase appears on increasing the probe concentrations further as shown in Fig. 4 for a DPPC bilayer containing two probe molecules per 32 lipid molecules. This effect is

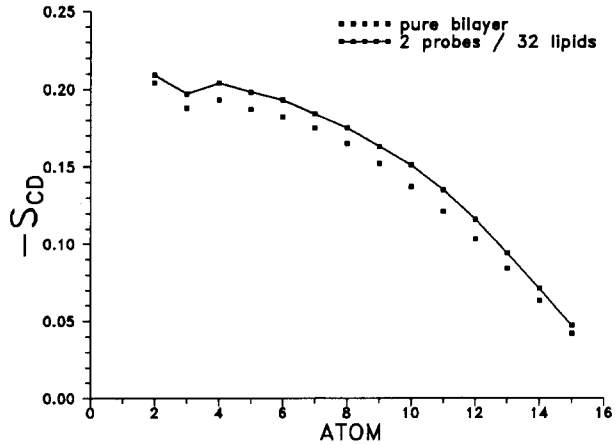

Fig. 4. The effect of the presence of probe molecules anchored at the aqueous interfaces of the DPPC bilayer on the order parameter profile of the C–D bonds along the hydrocarbon chains.

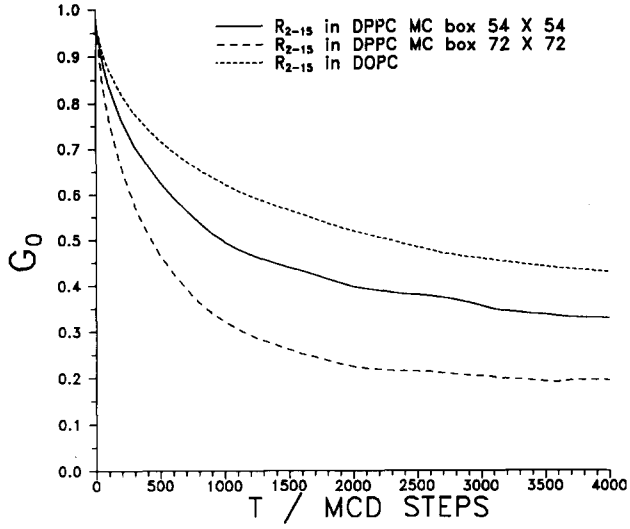

Fig. 5. The decay of the orientational correlation functions G_0 (see text) of the vectors connecting atoms 2 and 15 of the hydrocarbon chains in bilayers of DPPC and DOPC.

akin to that induced by cholesterol molecules in lipid bilayers. Indeed, we have previously reproduced the effects of cholesterol on the order parameters by introducing these probe molecules into lipid bilayers up to a molar ratio of 1:1 [10]. On the other hand, a small decrease in the order parameter of the first seven atoms is observed in DOPC bilayers at a 1:32 probe to lipid concentration. The effect is reversed on doubling the probe concentration, leading to a small increase in the order parameter profile across the whole chain.

The simulations thus indicate that the structural perturbations to the bilayer caused by the presence non-interacting probe molecules at experimental molar ratios of less than 1:100 are at best marginal and too small to be observed in measurements of the order parameter profiles.

3.4. Pure lipid bilayer – dynamic properties

In order to gain insight into the dynamic properties of the lipid chains which are monitored by the probe molecules, we shall now consider the rotational motions of large chain segments. The orientational time correlation function $G_0(t)$ for the vectors R_{2-15} joining atoms 2 and 15 in chains of DPPC and DOPC are shown in Fig. 5. The correlation function decays to a constant plateau at long time whose level is given by S^2, with S the corresponding order parameter of the vector. The correlation functions shown in Fig. 5 were calculated for bilayers of DPPC and DOPC. They decay faster and the level of the long time plateau drops on increasing the size of the Monte Carlo box, indicating that the orientational order decreases and the rotational rates increase on increasing the effective area per molecule of the lipid chains.

3.5. Perturbation of bilayer dynamics by probe molecules

The decay behaviour of the orientational time correlation functions for the chain segments shown in Fig. 5, is not affected by the presence of probe molecules at a molar concentration of 1:32 lipid molecules within the level of the statistical uncertainties. The simulations thus indicate again that the incorporation of non-interacting probe molecules in the bilayer structure causes minimal perturbations to the lipid chain dynamics.

3.6. Probes in lipid bilayers – dynamic properties

We shall here analyze the correlation functions $G_{k0}(t)$ calculated from the trajectories in the conventional way by fitting them to the predictions of physical models for rotational motions. The solution provided by the motional model can now be validated by comparing the extracted order parameters with the ones obtained directly from averaging along the trajectories. Order parameters, such as $\langle P_2 \rangle$ and $\langle P_4 \rangle$, can be calculated in a straightforward way from the number density obtained from the simulations (Fig. 2).

We now note that the number densities found for all the bilayer systems investigated here and the corresponding order parameters are inconsistent with the orientational order postulated by the 'wobble-in-cone' model. The cone angle of around 50° extracted from $\langle P_2 \rangle$ is clearly too small to account for the number density (Fig. 2). This model will therefore not be considered further.

The BRD model using the orienting potential of Eq. 1, yields unsatisfactory fits to the correlation functions (Fig. 6), for all the bilayer systems studied here. On the other hand, the order parameters $\langle P_2 \rangle$ and $\langle P_4 \rangle$ ex-

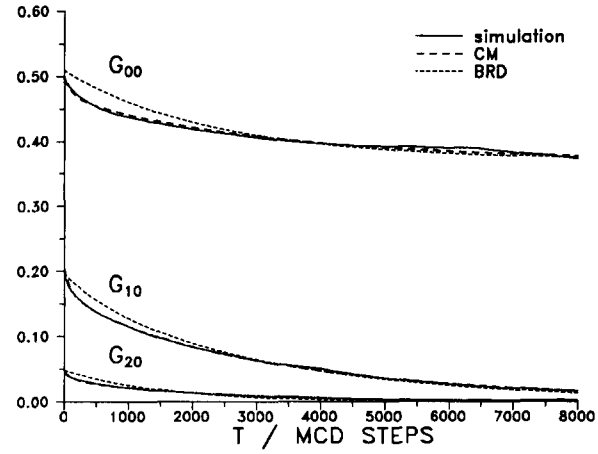

Fig. 6. The decay of the orientational correlation functions G_{k0} (see text) of the long axes of the probe molecules relative to the normal to the surfaces of a DPPC bilayer. Shown are the decays calculated from the MCD simulations and the fits obtained form the CM and BRD models. The model parameters extracted from the fits are given in Table 1.

Table 1
Model parameters extracted from a non-linear least squares fit to the orientational time correlation functions G_{k0}

Model	$\langle P_1 \rangle$	$\langle P_2 \rangle$	$\langle P_3 \rangle$	$\langle P_4 \rangle$	$D_c = \tau^{-1}$ (MCD steps)$^{-1}$	$D_\perp$ (MCD steps)$^{-1}$
Simulation	0.842	0.613	0.406	0.256		
BRD	0.0	0.609	0.0	0.248	–	$4.4 \cdot 10^{-4}$
CM inside cavity	0.961	0.887	0.675	0.656	$3.1 \cdot 10^{-2}$	
CM cavity in bilayer	0.868	0.676	0.495	0.356	–	$2.6 \cdot 10^{-4}$
CM overall order	0.834	0.600	0.334	0.234		

tracted from the analysis are in excellent agreement with those obtained from the trajectories (Table 1).

Only the recently proposed CM model [8,9] provides a good fit of both the decay of the correlation functions (Fig. 6), and the order parameters (Table. 1). As expected the order parameters are found to decrease on increasing the effective area per molecule with a concomitant increase in the rotational diffusion coefficients.

The CM model for the motion of the probe molecules is based on the free-volume hypothesis formulated above. Here the probe molecules are assumed to rattle fast within a cavity which itself undergoes a slow rotational diffusion in the bilayer structure. The fast rattling motions may be identified with motions within free-volume cavities between the lipid chains. The cavities themselves change their orientation relative to the bilayer normal due to the internal conformational motions of the lipid chains. Thus, in the spirit of the free-volume hypothesis for orientational order, we expect that the orientational motions of long chain segments determine the slow motions of the cavities in the CM model. In order to check this, we have evaluated the correlation function $G_0(t)$ but taking into account only the slow motion of the probe molecules using the parameters extracted from the CM model. These functions are shown in Fig. 7a together with the correlation functions corresponding to the motion of long chain segments in DPPC bilayers. The correlation function for the interatomic vector R_{2-15} for the DPPC

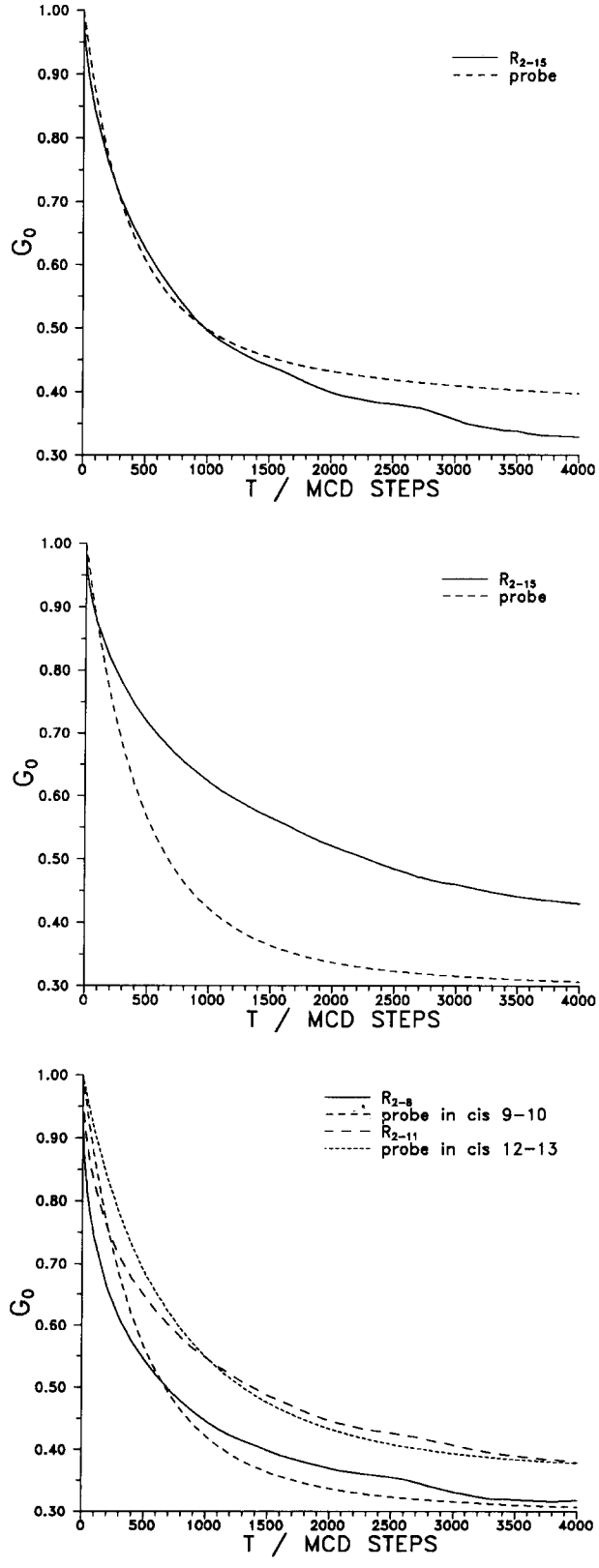

Fig. 7. (a) The decay of the orientational time correlation functions G_0 (see text) of the vector connecting atoms 2 and 15 of the hydrocarbon chains in bilayers of DPPC and of the long axes of the probe molecules embedded in the bilayer. (b) The decay of the orientational time correlation functions G_0 (see text) of the vector connecting atoms 2 and 15 of the hydrocarbon chains in bilayers of DOPC and of the long axes of the probe molecules embedded in the bilayer. (c) The decay of the orientational time correlation functions G_0 (see text) of the vector connecting atoms 2 and 8 in DOPC bilayers (*cis* unsaturated segment at position 9–10) and the vector connecting atoms 2 and 11 in bilayers of lipids with a *cis* unsaturated segment at position 12–13 and of the long axes of the probe molecules embedded in the bilayers.

chains decays on the same time scale as that for the long axis of the probes. Moreover, the two functions decay to the same long time plateau, thus indicating a similar orientational order relative to the normal to the bilayer plane. A similar behaviour is observed for DMPC bilayers and the saturated palmitoyl chains in POPC bilayers.

In marked contrast, the correlation function for R_{2-15} in DOPC bilayers (Fig. 7b), and the oleoyl chains in POPC bilayers exhibited a markedly slower decay than that for the long axes of the probes. Furthermore, the correlation function for the vector decays to a significantly higher long time plateau than that for the probe axes. Interestingly, the behaviour of the correlation function for the vector R_{2-8}, which does not span the unsaturated segment (Fig. 7c), is similar to that observed for the probe molecules. This is in agreement with the finding above of similar order parameters for these vectors and the long axes of the probes.

In trying to rationalize the probe behaviour in POPC and DOPC bilayers one has to bear in mind that the introduction of a *cis*-unsaturated double bond segment into a polymethylene chains modifies the conformational dynamics of the chain. It has been previously shown using Brownian Dynamics [13] and Monte Carlo dynamics [12] simulations on isolated hydrocarbon chains, that the rigid *cis* segment containing four atoms undergoes significantly slower rotational motions than the two saturated segments attached to it. In addition, these two segments undergo faster conformational motions than the corresponding segments in a long saturated hydrocarbon chain. The rate of rotational motion of any interatomic vector spanning the double bond, however, is determined by slow motion of the rigid *cis* segment. The slow decay of the correlation function for the vector R_{2-15} for the unsaturated chains in the POPC and DOPC systems thus reflects the slow and restricted motion of the *cis* segments in the bilayers.

The results here indicate that the probe molecules monitor the conformational motions of the short saturated segments attached to the rigid *cis* segment rather than of those of the long chain axes. This can be understood in view of the fact that the faster moving saturated chain segments determine the changes in the free-volume cavities in the bilayer structure. Following this reasoning, we would expect the probe molecules to monitor the motion of long chain axes if the *cis* segment is situated near the end of the lipid chains. In order to test this idea, we have carried out simulations for a bilayer containing lipid chains with *cis* double bonds at the 12–13 position. We indeed find that the correlation function for the vector R_{2-11} is in good agreement with that observed for the long chain axes, Fig. 7c. Again, significant discrepancies are observed between the correlation function for the vector R_{2-15} which spans the unsaturated segment and that for the long axes of the chains. We thus believe, that the probe molecules reflect the motion of the saturated segments only in the POPC and DOPC bilayer systems. This in contrast to the dynamically homogeneous saturated systems of DMPC and DPPC.

4. What do probe molecules monitor in lipid bilayers?

The simulations presented above support the conventional prescription for describing the orientational behaviour of probe molecules in lipid bilayers in terms of a local effective orienting potential. They indicate, however, that the potential arises from the confinement of the probe molecules between long segments of lipid chains in elongated free-volume cavities within the bilayer structure. In this sense the orienting potential concept needs to be refined in order to take into account the combined effect of the restricted free rattling motions of the probes within the free-volume cavities and the orientations of the cavities themselves relative to the normal to the bilayer plane. The time scale of the motions of the cavities within the bilayer is determined by the rotational motions of long segments of the lipid chains.

This separation of motional modes forms the key to answering the question as to what physical processes the probe molecules monitor within the lipid bilayer structure. It was shown above that the widely used BRD model which assumes that the probe molecules move within a simple orienting potential does not account for the decay of the time correlation functions yielded by the simulations. On the other hand, the CM model, which explicitly includes the fast motions within the cavities as well as the slow reorientations of the cavities in the bilayer structure correctly describes the correlation function decays. Interestingly, this model was originally invoked in order to provide a consistent framework for the interpretation of fluorescence depolarization experiments on TMA-DPH molecules incorporated in lipid vesicles and multibilayer systems [9]. It was shown that the time-resolved fluorescence depolarization and anisotropy decays, which are in fact described by the time correlation functions $G_{k0}(t)$ of Eqs. 2 and 3, contain interwoven fast and slow components such as are expected to arise from a superposition of motional processes. The CM model has the merit that it provides a way of unravelling the two processes and laying a relation between the slow modes of motion of the probe molecules and the dynamic behaviour of the lipid chains.

The simulations show that the ideal probe molecules cause at most a marginal perturbation of the intrinsic orientational behaviour of the lipid molecules at the low concentration levels commonly used in experi-

ments. Nevertheless, one has to bear in mind that while the probe molecules indeed monitor the orientational fluctuations of saturated lipid chains, their behaviour in the bilayer system does not reflect the motions of *cis* unsaturated segments. Rather, the probe monitor the behaviour of the saturated chain segments attached to the central double bond. It was shown above that the timescale of motions and order parameters of long saturated chain segments corresponded closely with those extracted for the slow motional processes from the CM model. These observations justify the use of rigid probe molecules such as TMA-DPH and Cholestane spin labels for monitoring the orientational order and dynamics in lipid bilayer systems.

References

[1] Zannoni, C., Arcioni, A. and Cavatorta, P. (1983) Chem. Phys. Lipids 32, 179–250.
[2] Nordio, P.L. and Segre, U. (1979) in The molecular physics of liquid crystals (Luckhurst, G.R. and Gray, G.W., eds.), pp. 411–426, Academic Press, New York.
[3] Evans, M., Evans, G.J., Coffey, W.T. and Grigolini, P. (1982) Molecular Dynamics, Wiley, New York.
[4] Cukier, R.I. (1974) J. Chem. Phys. 60, 734–743.
[5] Cukier, R.I. and Latakos-Lindenberg, K. (1972) J. Chem. Phys. 57 3427–3435.
[6] Kinosita Jr., K., Kawato, S. and Ikegami, A. (1977) Biophys. J. 20, 289–305.
[7] Kinosita Jr., K., Kawato, S. and Ikegami, A. (1984) Adv. Biophys. 17, 147–203.
[8] Van der Sijs, D.A., Van Faassen, E.E. and Levine, Y.K. (1993) Chem. Phys. Lett. 216, 559–565.
[9] Van der Heide, U.A., Van Zandvoort, M.A.M.J., Van Faassen, E.E., Van Ginkel, G. and Levine, Y.K. (1994) J. Fluorescence 3, 269–277.
[10] Van der Sijs, D.A. and Levine, Y.K. (1994) J. Chem. Phys. 100, 6783–6789.
[11] Levine, Y.K., Kolinski, A. and Skolnick, J. (1993) J. Chem. Phys. 98, 7581–7587.
[12] Levine, Y.K. (1993) Molec. Phys. 78, 619–628.
[13] Rey, A., Kolinski, A., Skolnick, J. and Levine, Y.K. (1992) J. Chem. Phys. 79, 1240–1249.
[14] Rose, M.E. (1957) Elementary theory of angular momentum, Wiley, New York.
[15] Seelig, A. and Seelig, J. (1974) Biochemistry 13, 4839–4845.
[16] Seelig, A. and Seelig, J. (1977) Biochemistry 16, 45–50.
[17] Rance, M., Jeffrey, K.R., Tulloch, A.P., Butler, K.W. and Smith, I.C.P. (1980) Biochim. Biophys. Acta 600, 245–262.
[18] Cevc, G. and Marsh, D. (1987) Phospholipid Bilayers: Physical Principles and Models, Wiley, New York.
[19] Small, D.M. (1986) The Physical Chemistry of Lipids, Plenum, New York.
[20] Silver, B.L. (1985) The Physical Chemistry of Membranes, Solomon, New York.
[21] Houslay, M.D. and Stanley, K.K. (1982) Dynamics of Biological Membranes, Wiley, Chichester.
[22] Seelig, J. and Waespe-Šarčevic (1978) Biochemistry 17, 3310–3315.
[23] Fringeli, U.P. (1977) Z. Naturforsch. Teil C 32, 20–24.
[24] Korstanje, L.J., Van Faassen, E.E. and Levine, Y.K. (1989) Biochim. Biophys. Acta 980, 225–233.
[25] Johansson, L.B.-Å, Lindblom, G., Wieslander, A. and Arvidson, G. (1981) FEBS Lett. 128, 97–99.
[26] Van de Ven, M., Kattenberg, M., Van Ginkel, G. and Levine, Y.K. (1984) Biophys. J. 45, 1203–1210.
[27] Binder, K. (1986) Monte Carlo Methods in Statistical Physics, Springer-verlag, Berlin.